5ICEGE
5th International Conference on Earthquake Geotechnical Engineering
January 2011, 10-13 | Santiago, Chile
Paper No. SAOTA

SEISMIC ANALYSIS OF A LARGE GRAVITY QUAY WALL OF COMPLEX GEOMETRY USING A SIMPLIFIED APPROACH

Merrick TAYLOR [1], Ian FELTHAM[2], Zygmunt LUBKOWSKI[3], Robert MAY[4]

ABSTRACT

This paper presents the seismic evaluation of an existing large gravity quay wall of varying geometry using a performance based framework. It features the application of a simplified 3-D analysis procedure developed to assess the global wall stability using the concept of "linked 2-D slices" in preference to a complex 3-D finite element approach. The linked 2-D slice procedure was further developed to enable estimates of performance of the wall under seismic events, including tilting and sliding displacements using simple rigid block models. The results from the structural appraisal aided in developing scenarios of possible wall deformations, which were assessed in turn to bound the likely performance, enabling comparison to pre-defined performance targets established by the Client. A novel procedure to develop the pseudostatic loads for stability analyses of large walls based on Peak Ground Velocity of the dynamic load is also presented and compared to published recommendations in the literature.

Keywords: Retaining Wall, Dynamic Analysis, 3-D stability, Performance Based Design

INTRODUCTION

This paper presents the application of a seismic analysis of a retaining structure with complex 3-D geometry using a simplified method based on the concept of "linked 2-D slices". The method for assessing static stability is extended to estimate performance under low probability seismic events with the assessment of co-seismic displacements. Specific details of the project have been removed to retain Client confidentiality.

The quay wall considered is a large mass concrete gravity retaining structure constructed *circa* 1900. Figure 1 presents an isometric view of the wharf structure. It is approximately 200 m long, varying in height from 17.5 m at either end of the wall to a maximum height of 36.5 m in the centre at the deepest section of the wharf, where it transects a buried valley. This variation occurs over approx. 50 m length, with wall widths varying between approximately 8.4 m and 14 m. The variation of section width and height are on account of the method of construction being modified in a somewhat *ad hoc* manner in response to encountered ground conditions on site. The varying geometry provided a challenge in adopting simplified 2-D slice analysis methods to assess the overall wall reliability and performance.

The role of the structure has changed to service modern vessels with hazardous material requirements, requiring demonstration of its reliability for the foreseeable future, taking into consideration extreme environmental loads that include earthquakes. A scoping study in which critical sections through the wall were assessed via a simple 2-D slice assessment had indicated insufficient level of stability against the

[1]PhD Candidate, University of Canterbury, Christchurch, New Zealand (formerly Geotechnical Engineer, Arup, London, UK); e-mail: merrick.taylor@pg.canterbury.ac.nz
[2]Associate Director, Arup, London, UK
[3]Associate Director, Arup, London, UK
[4]Technical Director, Atkins Global Ltd., Epsom, UK

code, and initial seismic assessment suggested insufficient stability under sliding and overturning failure modes at discrete sections of the wall (analysed in 2-D). The analyses in this paper were commissioned in order to investigate the quay wall stability and account for any benefit afforded the weaker sections of the wall by adjacent stronger sections. Ultimately the aim was to confirm whether or not retrofit works were required. The analysis philosophy was influenced by published documentation that provides guidance on assessing existing structures not designed to modern codes (IStructE 1996, ASCE 41-06) in addition to codes, published guidelines and state of the art papers covering seismic analysis aspects (e.g. PIANC 2001, ASCE 4-98, Eurocode 8).

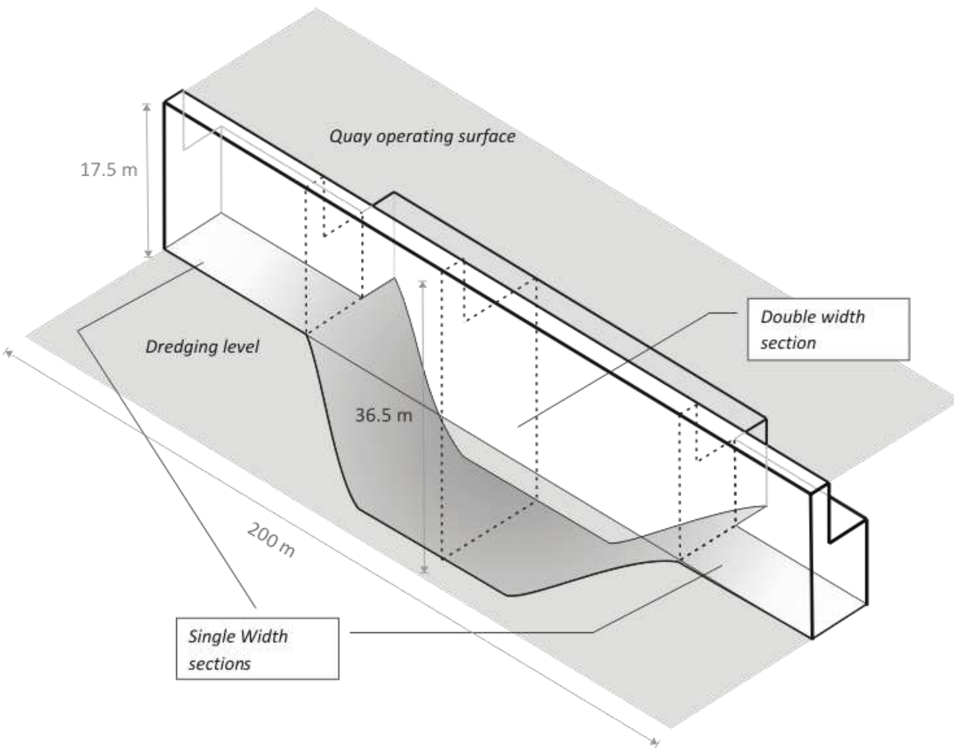

Figure 1: Isometric schematic of the 3-D geometry of the wall structure

SEISMIC LOADING & DESIGN PHILOSOPHY

The purpose of the seismic analysis is principally to test structure robustness under an extreme load condition. The "test-level" or Design Basis Event (DBE) required by the Client for this project was based on a maximum acceleration (a_{max}) on rock of 0.25g, corresponding to a scenario earthquake of approximately M_w 6.0 occurring within close proximity of the site (< 10 km). As it was never designed to account for seismic loading, this presents a very onerous load case for the structure considered. A spectral shape for this hypothetical event was fitted to the design a_{max} and spectrally compatible accelerograms of appropriate duration and energy content were used for the dynamic analysis.

In addition to the DBE, the Client required consideration of a Safety Margin Event (SME) termed a "cliff edge" scenario, where the DBE is exceeded by +40% to assess the sensitivity of the structure to a larger dynamic load. Thus the SME has an a_{max} value of 0.35g. The aim being to ensure a brittle or catastrophic failure doesn't occur within the range of the potential uncertainty on the DBE, although the +40% figure is based on judgment rather than a strict probabilistic basis. This two-level design criterion was viewed as complementary to the performance based design methodology in terms of considering multiple environmental load levels with corresponding performance targets. This philosophy has become the means by which seismic design is routinely conducted in modern civil engineering practice.

Defining performance requirements and key assumptions

In considering the acceptability or otherwise of the induced deformations of the wall predicted from the seismic analysis, the PIANC (2001) guidance is particularly relevant and provided the framework by which the performance was evaluated. The design events (i.e. DBE, SME) and corresponding performance grades were changed from those specified by PIANC to reflect the specific requirements of the project and were agreed with the Client and their expert advisors. Table 1 presents the tolerated permanent wall deformations corresponding to the respective design events.

Table 1: Performance grades and corresponding targets for the quay walls:

Level of Damage	Safety Case Earthquake	
	DBE* [a_{max} = 0.25g]	SME* [a_{max} = 0.35g]
Normalised residual horizontal displacement (d/H)**	Less than 1.5%	5-10%
Residual tilting towards the sea	Less than 3°	5-8°

*DBE = Design Basis Event; SME = Safety Margin Event (DBE + 40%)
**d: residual displacement at top of the wall. H is the height of the wall.

The performance requirements were considered in light of the assumed behaviour of the wall at the Ultimate Limit State (ULS): That a pre-existing crack at the base of the wall allows translation or rotation freely, without any contribution from the tensile strength of the concrete or rock foundation. The advantages of this assumption are firstly that the consequence of brittle failure of the mass concrete is considered preemptively, and secondly that mobilisation of active earth pressure may be considered for the ULS. Thus the deformations considered are for the rigid body displacement of the wall mass; fitting the modes of deformation for a gravity retaining structure, rather than a fixed-base embedded-wall (NB: This latter scenario was also considered but produced lower co-seismic displacements). Consideration of the effects of wall displacements on quay cranes was beyond the scope of our investigation and is the subject of further study.

ANALYSIS PROCEDURE

Dynamic response of wall

The seismic analysis procedure essentially followed that outlined by Steedman (1998). In addition, Eurocode 8 part 5 (EC8) and other documentation was used as guidance for undertaking the simplified analysis. Before initiating pseudo-static calculations, an assessment of how the incoming ground motion affects the wall response is required as amplification and phase effects have been shown to have a significant effect on dynamic earth pressures (Steedman and Zeng, 1990). Additionally EC8 recommends site response analysis for walls in excess of 10 m in height. This is especially important due to the limitations of pseudostatic earth pressure theory that considers uniform inertia applied to the backfill. Additionally, the backfill has two soil strata with distinctly different stiffness properties – a soft *in situ* marine alluvium (shear wave velocity, V_s ~ 150 m/s) immediately overlying rock (V_s ~ 1600 m/s), with compacted granular fill comprising the upper approx. 10 m of the wall backfill (V_s ~ 270 m/s). With the moderate ground motions considered, some soil non-linearity was anticipated in the alluvium, which would have the advantage of damping high frequencies, but amplifying low frequency motions at the natural period of the wall backfill.

A 2-D site response in explicit dynamic finite element code *LS-DYNA* (Hallquist, 2006) was conducted at two wall section heights – maximum height of 36.5 m and at a transition height of 22 m, where the wall section changed in depth between narrow and wide sections of the wall. The constitutive model used for both soils was a simple non-linear stiffness multi-yield plasticity model, with hysteresis governed by the extended Masing Criteria (Kramer, 1996). Both backfill soils had been shown to have low susceptibility to build up of excess pore water pressures in cyclic direct simple shear and triaxial testing. A more sophisticated constitutive model was therefore not deemed necessary.

Results from the dynamic analyses indicated a simple relationship between incoming ground velocity and dynamic thrust could be used as a basis to derive the effective horizontal acceleration applied to the wall for pseudostatic analyses (refer Figure 2). This was principally on account of the large wall height where the maximum positive acceleration in the backfill responsible for driving the dynamic thrust, at any moment during the earthquake, would be the integral of the acceleration time history. Hence peak thrust correlated directly to peak ground velocity (v_{max}).

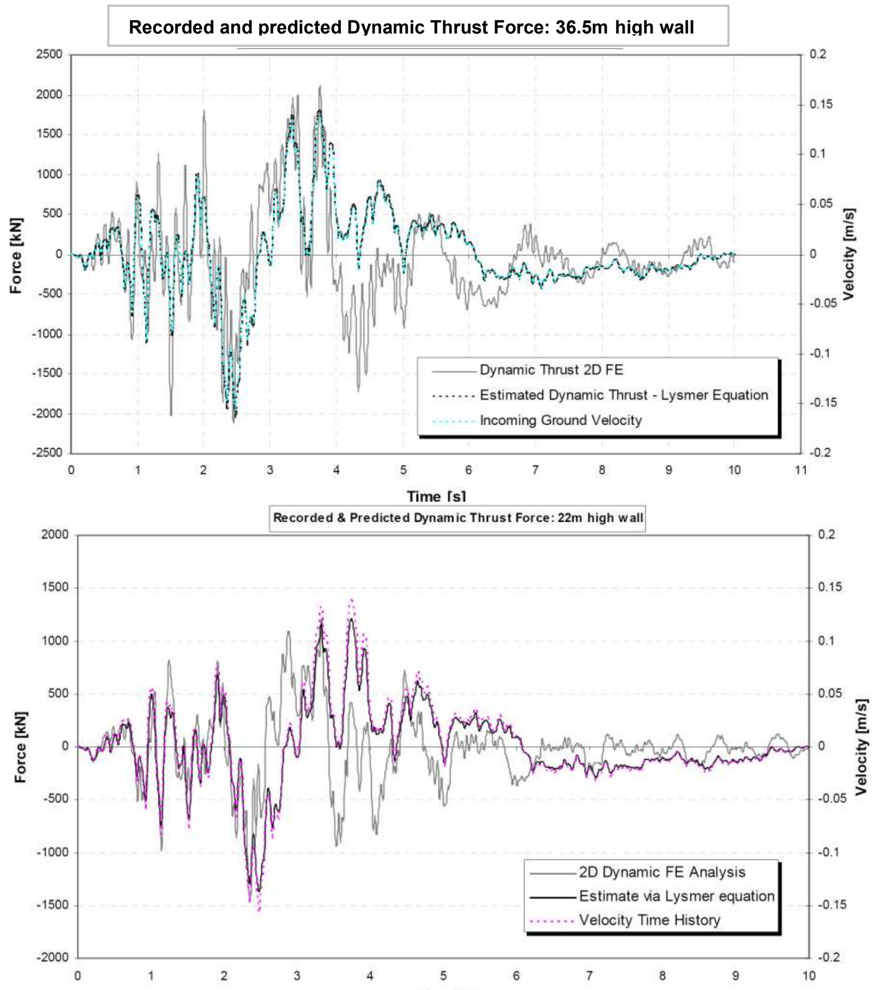

Figure 2. Output horizontal force resultant time history compared to prediction using modified Lysmer equation and incoming velocity time history (a) 36.5m wall height (b) 22m wall height

The relation presented by Lysmer and Kuhlemeyer (1969) was found to be directly applicable to the wall as a whole to relate incoming velocity to applied shear stress, and hence total thrust on the wall. Additionally, from the method for determining the peak thrust for rigid walls derived by Wood (1973), the following relation was used to back-calculate the effective horizontal acceleration, $k_{h(eff)}$ affecting the wall, anywhere along its length, as a function of wall height as:

$$k_{h(eff)} = \frac{v_{max} \cdot V_{s,ave}}{H \cdot g} \quad (1)$$

Where $V_{s,ave}$ is the average shear wave velocity of the wall backfill (m/s), H the height of the wall (m), and g is gravity (m/s^2). Note that this in itself does not account for amplification of ground motion in the backfill, and plots in Figure 2 indicate amplification occurred to long period motion not accounted for by the estimate proposed, but crucially not affecting the estimate of peak thrust.

This approach has been compared favourably to a recent National Cooperative Highway Research Program (NCHRP) study presented by Anderson et al. (2008) to assess the effect of "wave coherency or scattering effect" on typical wall geometries. They evaluated the 2-D site response of a range of wall heights. This formed the basis for recommendations of an appropriate reduction factor for determining design horizontal acceleration (i.e. $k_{h(eff)}$) as a function of wall height, and design spectral shape (ratio of spectral accelerations at 1 Hz (S1) to a_{max}; a rough proxy for frequency content of the ground motion) including site class effect (i.e. simple representation of site stiffness). This correlation is perhaps not too surprising; Kramer (1996) notes that the ratio v_{max}/a_{max} should be related to frequency content, and $2\pi(v_{max}/a_{max})$ may be interpreted as the period of vibration of an equivalent harmonic wave, indicating the period of ground motion that is most significant. Where use of equation (1) results in significant deviation from the NCHRP recommendations is for smaller wall heights where use of v_{max} will begin to over-predict the ground motions that may affect a wall. The peak thrust on the wall will become increasingly dominated by a_{max}. Figure 3 presents the comparison.

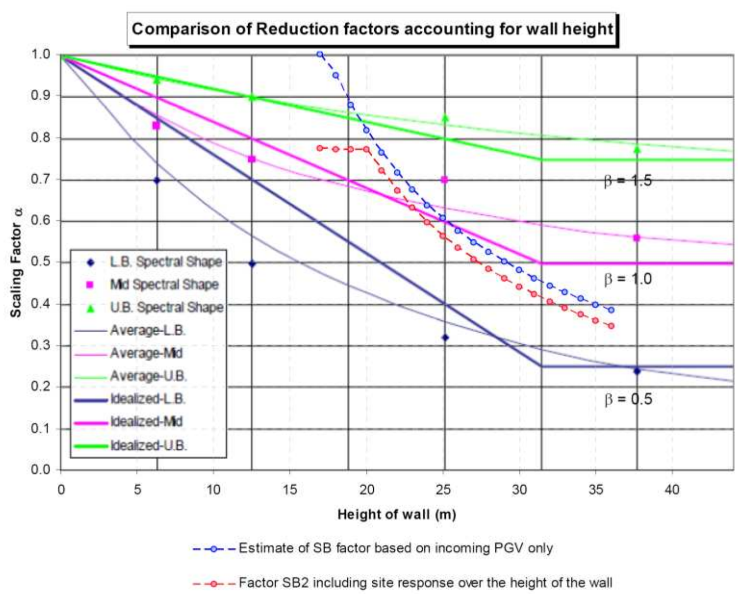

Figure 3. Comparison of proposed estimate for effective design acceleration for large retaining structures based on v_{max} (PGV), modified after Anderson et al. (2008).

PSEUDOSTATIC 2-D SLICE ANALYSIS

Methodology

The seismic 2-D slice analysis conformed to the limit equilibrium approach. Sliding, overturning and bearing failure modes were considered in addition to structural checks. This paper focuses on the sliding and overturning modes, the latter of which governed wall behaviour. The EC8 recommendations for dynamic earth pressures were generally followed assuming the wall translated sufficiently to develop active earth pressures under dynamic loading at the ULS, i.e. Mononobe-Okabe (Seed and Whitman, 1970). The dynamic load reduction factor r in EC8 was set to 1.0 as displacements via dynamic rigid block analyses would be calculated directly.

Analysis results

All 2-D slice sections of the wharf analysed were found to have F_s for the seismic load case of less than 1.0 for overturning, and greater than 1.0 for sliding mode. Figure 4 presents safety factor profiles along the length of the wall. Changes observed are as a result of geometrical irregularity. As the overturning F_s was less than unity, by definition the bearing capacity is considered insufficient as this implies that the point of action of the weight force of the wall is outside the foundation extent, albeit momentarily.

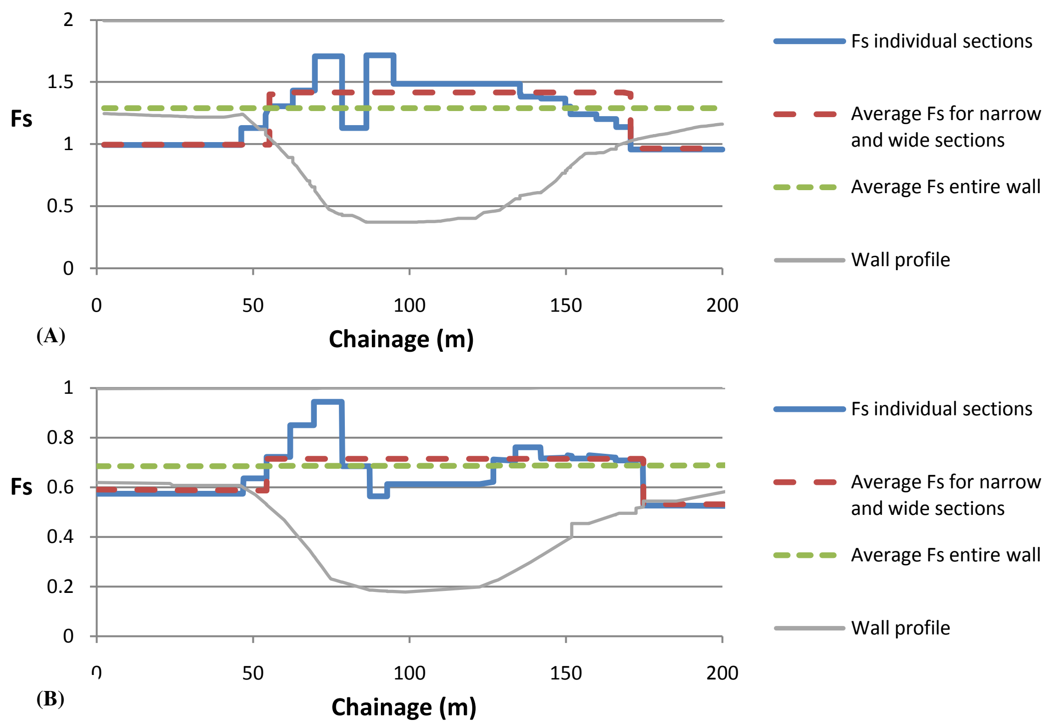

Figure 4. Factors of Safety under DLE (A) Sliding, and (B) Overturning.

LINKED 2-D SLICE ANALYSIS

Development and implementation

The concept of linking 2-D slices has been developed for the retaining structure based on earlier work to evaluate 3-D slope stability by simplified means. Baligh and Azzouz (1975) used moments to define the 3-D factor of safety, $F_{S,3D}$, with a projection correction to account for the difference between the projected area of the slip plane for a 2-D cross section and the actual area of the 3-D slip surface (refer Figure 5A). This concept was adopted by Loehr et al. (2004) for their weighted resistance approach, where the results from n number of 2-D slip circle analyses were summed together. The weighted average method developed for the retaining structure was based on a combination of the aforementioned methods. It was necessary to modify the form of the equation from earlier approaches as non-regularly spaced slices were considered to better capture the observed changes in wall geometry.

The wall was divided into 15 No. discrete lengths that may be approximated in the analysis by a single 2-D slice running through the centre of each. The F_S for each 2-D slice is then multiplied by a corresponding projection correction (d_s) to account for the actual surface area of the failure plane for the discrete length (d_x) considered. The results of these single 2-D slice analyses are then summed and divided by the length of the wall to obtain the weighted average $F_{S,3D}$ for the wall as a whole:

$$F_{S,3D} \cong \frac{\sum_{i=1}^{n}(F_{S,i} \times d_{s,i})}{\sum_{i=1}^{n} d_{x,i}} \quad (2)$$

Where $F_{S,i}$ is the factor of safety for the i^{th} cross section, $d_{s,i}$ the actual slip dimension of the i^{th} cross section, $d_{x,i}$ the projected dimension of the i^{th} cross section assumed by a 2-D slice analysis. In the case considered, connections of the end-wall sections to other walls at the port were conservatively ignored, largely for simplicity, although it is appreciated that end wall connections may provide additional support. This approach was found to provide a reasonable estimate of the $F_{S,3D}$ when the variation between the F_S values of the component slices is small, but could produce undesirable deviation from the actual $F_{S,3D}$ if significant variations existed. The actual $F_{S,3D}$, if calculated directly using the respective components of driving, F_D, and resisting forces, F_R, is as follows:

$$F_{S,3D} = \frac{\sum(F_{R,i}d_{s,i}+F_{R,i+1}d_{s,i+1}+\cdots+F_{R,n}d_{s,n})}{\sum(F_{D,i}d_{s,i}+F_{D,i+1}d_{s,i+1}+\cdots+F_{D,n}d_{s,n})} \quad (3)$$

Moments may be similarly added, but not directly from individual 2-D slice calculations. The following section presents how this may be achieved.

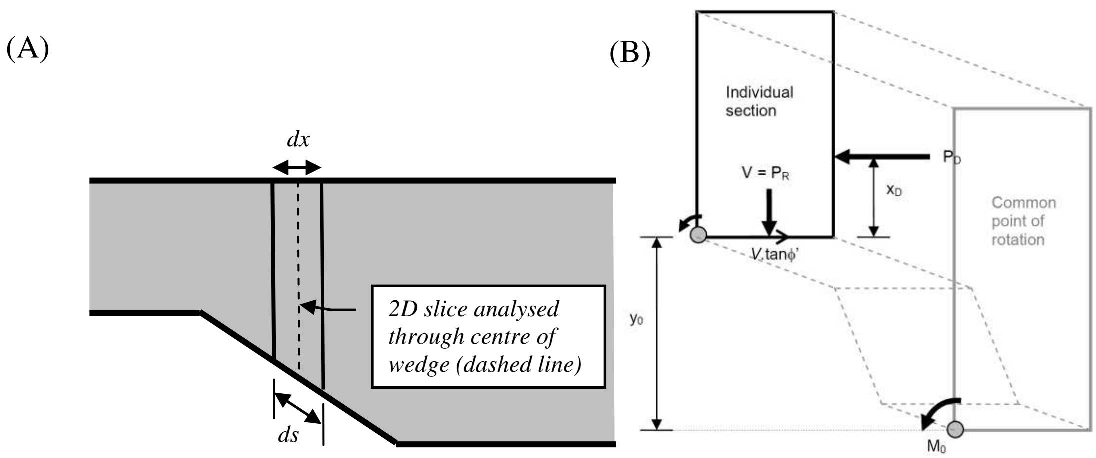

Figure 5: (A) Projection correction of Baligh & Azzouz, applied to change in retaining wall geometry(B) Reference diagram for the transformation of individual section moments to a new point of rotation at vertical offset y_0.

Common point of rotation.

The linked 2-D analysis as presented above, when applied to the overturning mode using results of independent 2-D slice analyses; require further processing in order to obtain a F_S against overturning about a common point of rotation. Figure 6B presents the applied driving and resisting resultant moments and forces for a section of wall in relation to a new point of rotation (say for the base of the deepest section of the wall). To calculate the moments at a new reference point for overturning (i.e. the base of the maximum height of the wall) the following transformation from local to global point of rotation is required for offset sections:

$$M_{0D,i} = P_{D,i} \cdot (x_{D,i} + y_{0,i}) - \Phi_i V_i \tan\phi \cdot y_{0,i} \quad (4)$$

$$M_{0R,i} = P_{R,i} \cdot x_{R,i} \quad (5)$$

where: $M_{0D,i}$ = driving moment of the i^{th} section about new point of rotation for the 3-D wall being considered.

$P_{D,i}$ = driving resultant force at the i^{th} cross section due to remaining components in equilibrium equation (whether positive or negative driving force).
$x_{D,i}$ = theoretical point of action of P_D
$y_{0,i}$ = vertical distance from the base of the 2-D slice and the new point of rotation.
Φ = mobilisation factor on the basal sliding resistance.
$V_i.\tan\phi'$ = sliding resistance along the base of the individual 2-D slice, where the i^{th} slice base level is less than the global wall rotation depth.
$M_{0R,i}$ = resisting moment of the i^{th} section about new point of rotation (unaffected).
$P_{R,i}$ = resistance resultant force at the i^{th} cross section due to weight of gravity wall structure only. The resisting force resultant in this case does not include sliding resistance at the base of the wall as it has no lever arm acting.
$x_{R,I}$ = theoretical point of action of P_R

The sliding resistance along the base of an individual slice is not mobilised in local moment resistance as it is in the plane of rotation and its point of action is zero. However, for the wall to rotate about the deeper point of action, this sliding resistance becomes engaged and must be considered in the analysis. At large offsets it may not be fully mobilised, and the net driving moment (Eq. 4) may reduce to zero. The mobilisation factor Φ controls the basal sliding resistance mobilised. This is calculated based on the amount of net driving force to available sliding resistance at an individual slice:

$$\Phi_i = F_{D,i}/F_{R,i} \qquad (6)$$

Note that the resistance to overturning is not increased by the offset. As formulated, the resistance comprises the restoring moment provided solely by the mass of the wall, whilst all other restoring moments (e.g. mobilised passive earth pressure at the wall toe, free body water pressure) were considered to contribute a negative driving moment. This also ensures the F_s is not inadvertently being applied to water at the front face, and prevents excessive passive earth resistance being considered at the ULS. While no specific guidance is provided on how the forces or moments are balanced in the limit equilibrium calculation in the legacy British Standards, the Spanish maritime code ROM0.5-05 presents this rational approach. Also, modern codes where partial factors are applied to shear strengths (e.g. BS 8002, Eurocode 7) avoid the factoring of water pressures, whilst only needing a global safety factor of unity to demonstrate compliance with the code.

Structural Evaluation

The key assumption of load transfer between adjacent sections was assessed in a simple structural analysis, using the resultant forces and moments obtained from the individual 2-D slice analyses. These were incrementally transferred in order to obtain uniform forces and moments applied to the wall as a whole at the ULS. This allows calculation of the implications of the redistribution of load along the length of the wall in terms of bending and shear induced in the structure. When balancing overturning moment, torsion is transferred to adjacent sections with relative ease, as the induced flexural stresses in the wall caused by this redistribution are small relative to the strength of the section. For sliding mode however, transfer of shear to produce a uniform factor of safety may induce significant moments in the wall, however if the F_s for all sections under static loading are well above what is required, any transfer is not considered necessary (as it would not be mobilised). The strength of each section was estimated assuming either no cracking or fully cracked before shearing, as there is uncertainty regarding the *in situ* condition of the quay wall in terms of the presence and persistence of any cracks that may be present. For brevity the details of the structural calculations are not presented in this paper.

PSEUDOSTATIC LINKED 2-D SLICE ANALYSIS

The linked analysis considered two scenarios of wall deformation:

1. The entire length of the wall remains intact and behaves as a single monolith
2. The wall cracks along joints between narrow and wide sections into 3 discrete wall sections.

For the first scenario the Linked 2-D slice method required coupling of all fifteen sections. The second scenario considered two slices joined together for one narrow-width end of the wall; one slice only for the opposite narrow-width end; and the remaining twelve slices linked together for the central large-width section of the wall. This was done in order to perform a tilting block analysis (Steedman and Zeng 1996). This analysis is analogous to the familiar Newmark sliding block concept (Newmark 1965) but for the tilting/ overturning mode of wall movement. It involves the calculation of the net overturning moment, and if at any time during the earthquake this net moment is greater than zero (i.e. equilibrium temporarily disestablished), then the angular acceleration of the wall, α becomes positive:

$$\alpha = \frac{M_D - M_R}{I_\theta} \tag{7}$$

Where M_D and M_R are the net driving and resisting moments respectively, acting on the wall at any given time. I_θ is the rotational mass moment of inertia of the wall. The latter is calculated for each scenario considered. Where α is positive it is integrated to obtain the angular velocity ω of the wall, after which the angle of wall rotation θ about the base is obtained by further integrating ω. Depending on the height of the wall, the final outward displacements at wall top may then be obtained by simple trigonometry. Important extensions to the rotating block method were implemented in the spreadsheet-based program used to perform these calculations. These are summarised as follows:

1. For $F_{s,3D}$ calculation, the analysis considers the rotation to be occurring about the base of the maximum height of the section. Thus for sections of wall that are less than the maximum height, H_{max}, basal sliding resistance becomes mobilised to resist overturning, providing a restoring moment (Figure 5B). This sliding resistance was assumed conservatively to be only acting when there is no rotational movement occurring. This assumption dramatically drops the critical acceleration temporarily, resulting in larger estimated displacements. In theory this reduction would not occur as sliding resistance is a function of the vertical force applied to the base not the basal contact area. However, sections not at full height may be dragged forward in order to maintain a uniform tilt angle, reducing certainty of sliding resistance acting on the base at these sections.
2. A global critical acceleration for the entire wall, k_{cr} is determined by using the 3-D F_s approach discussed previously.
3. Final displacements are estimated based on summed moments for the entire wall section being considered.
4. Mobilisation of passive earth pressure at the toe of the wall is included, such that increased passive resistance is mobilised progressively as the wall tilts outwards. This was calculated incrementally, and k_{cr} increases when this occurs. As each section of the wall had a different height of alluvium providing passive support to the toe of the wall, from 0 m at the ends of the wall to a maximum thickness of 22.5 m at the centre, each section would mobilise different proportions of passive earth pressure under uniform outward displacement. Therefore, for each section, a unique *p-y* curve was derived from the stiffness degradation properties of the alluvium.

Results of Linked 2-D slice dynamic analysis

Table 2 presents the estimated 3-D F_s values for the DLE event. Despite coupling together the sections of the wall, the F_s in overturning remains below unity, indicating permanent tilting displacements are expected to occur. The effect of considering a common point of rotation results in lower F_s. If wall friction is mobilised for sections offset from the common rotation depth, this raises the F_s for those scenarios where significant change in profile occurs, however in all cases the F_s remains below 1, indication overturning occurs; preventing the mobilisation of this sliding resistance due to momentary loss of basal contact.

Table 2: 3-D factors of safety - dynamic

Scenario	Sliding	Overturning		
		Moments about individual sections	Common point of rotation*	
			A	B
Entire length	1.28	0.68	0.49	0.89
End narrow sections (Sections 1-2)	1.00	0.59	0.52	0.52
Central wide sections (Sections 3-14)	1.40	0.71	0.58	0.77
End narrow section (Section 15)	0.96	0.53	0.52	0.52

*Taken about the base of the maximum height of the wall over length considered. Case A considers no sliding friction mobilised. Case B considers basal sliding friction partially mobilised at the overturning ULS.

For the overturning mode, internal torsions between adjacent sections are transferred to provide a uniform $F_{s,3D}$. The induced shear along the interfaces due to this transfer is plotted in Figure 7 and compared to the cracked and uncracked shear strengths. The results indicate that shear stress exceeds the cracked shear strength, particularly at interfaces between the narrow and wide sections, but does not exceed the limiting uncracked shear strength. The emphasis of the evaluation there shifted to assessing the consequences of whether the wall remains as a monolith throughout the earthquake or whether it cracks permitting independent movement between narrow and wide wall sections. This was done in order to bound the likely consequences of either scenario occurring:

- Assuming the wall remains as a monolith, and transfer of internal torsions along the entire length of the wall is unhindered.
- Assuming the wall develops cracks through the interface between narrow and wide wall sections, preventing further transfer of torsion between the separated sections of wall (ignoring any shear along the interface between blocks).

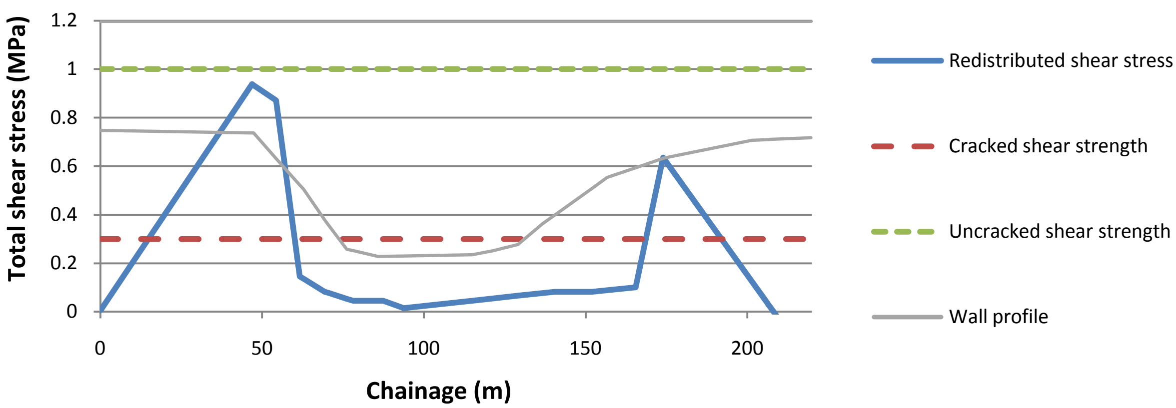

Figure 6: Implications of moment transfer in terms of induced shear stress in the wall

These simple scenarios formed the basis of the assessment of displacements under overturning mode. It avoids the complicated problem of assessing crack propagation through the wall at the interface between blocks. It is considered unlikely that sufficient energy would be present in the design earthquake considered to propagate a crack all the way through the wall, particularly since this maximum design load occurs momentarily, and will not be the same time during the earthquake over the entire length of the wall, but is assumed for simplicity of the assessment.

Critical Accelerations & Displacement Estimates

Figure 7 presents a plot of critical acceleration and factor of safety for the entire wall for overturning as it changes throughout an applied time history. The large swings in the critical acceleration are as a result of the loss of basal sliding contact when the wall tilts forward, whilst the progressive increase in critical acceleration throughout the time history is as a result of increased mobilization of passive earth pressure at the front of the wall due to the progressive outward displacements.

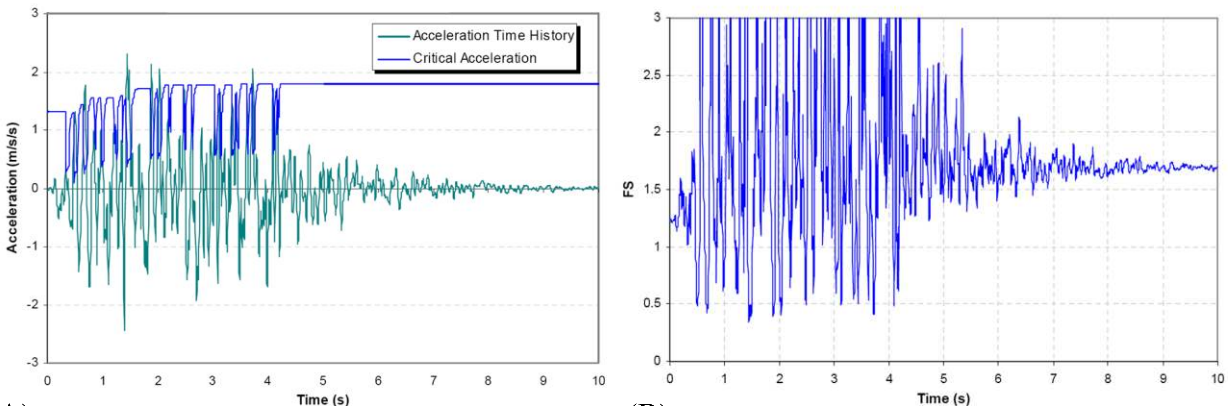

(A) (B)

Figure 7: (A) Critical acceleration (overturning) for entire wall compared to a design accelerogram (B) Pseudo 3-D factor of safety against overturning calculated for each time-step.

Clearly permanent displacements are anticipated. The temporary motion will involve outward tilting before coming to rest. Table 3 presents the range of calculated displacements for the scenarios considered for the wall for both the DBE and SME events. The calculated displacements in all cases are less than 200 mm (DBE) and 500 mm (SME), corresponding to d/H ratios of 0.5% and 1.4% (0.3° and 0.8°) respectively, and are less than the performance requirements for the wall stipulated in Table 1.

Table 3. Co-seismic displacements calculated for the wall

Scenario	Sliding Displacement [mm]		Overturning Displacement [mm]			
			Min		Max	
	DBE	SME	DBE	SME	DBE	SME
Entire Wall	0	0	120	250	190	500
End narrow sections (1&2 only)	<1	<1	90	220	130	340
Central wide sections (3-14)	0	0	60	140	70	180
End narrow section (15 only)	<1	<1	90	240	130	380
Wall with horizontal through-crack at 22.5m depth	<1	<1	40	100	50	150

CONCLUSIONS

This paper presents the application of a simplified method to assess the 3-D stability of a large retaining structure under both static and seismic loading, by means of “linked 2-D slices”. The method was extended to consider co-seismic deformations in order to assess performance of the structure under extreme loading scenarios. The structural appraisal provided a framework whereby possible wall deformation scenarios might be assessed to bound the likely performance. A thorough validation of the linked 2-D slices approach has not yet been conducted using either physical scale models or 3-D numerical analysis. Clearly this is an avenue of possible future research, however the method appears to provide a reasonable analytical means to estimate the 3-D stability relatively simply, and aid in the understanding of structural robustness under both static and extreme loading scenarios.

ACKNOWLEDGEMENTS

The first author would like to acknowledge the work of Mr. Domenico Pennucci (Arup) for the LS-DYNA analyses, and the project management of Mr. James Spencer (Pöyry Energy Ltd.).

REFERENCES

American Society of Civil Engineers. (2000) Seismic Analysis of Safety-Related Nuclear Structures and Commentary. ASCE, Reston, Virginia, ASCE 4-98.
American Society of Civil Engineers. (2007) Seismic Rehabilitation of Existing Buildings. ASCE, Reston, Virginia, 2007, ASCE 41-06.
Anderson D.G., Martin G.R., Lam I.P. & Wang J.N. (2008) Seismic Analysis & Design of Retaining Walls, Buried Structures, Slopes, & Embankments. Vol.1. NCHRP Report 611. Transportation Research Board, Washington D.C.
Baligh, M.M., and Azzouz, A.S. (1975) End effects on stability of cohesive slopes. Journal of the Geotechnical Engineering Division, 101, No.11, pp. 1105-1117.
CEN (2004). Eurocode 8: Design of structures for earthquake resistance — Part 5: Foundations, retaining structures and geotechnical aspects. European Committee for Standardization, Brussels, EN 1998-5.
Hallquist, J.O. (2006) LS-DYNA theory manual. Technical Report, Livermore Software Technology Corporation. Livermore, CA. Available at: http://www.lstc.com
Institution of Structural Engineers. (1996) Appraisal of Existing Structures. 2nd Ed. London.
Kramer, S.L. (1996) Geotechnical Earthquake Engineering, Prentice Hall, NJ, USA.
Loehr, J.E., McCoy, B.F., and Wright S.G. (2004) Quasi-Three-Dimensional Slope Stability Analysis Method for General Sliding Bodies. Journal of Geotechnical and Geoenvironmental Engineering, 130, No. 6, pp. 551-560.
Lysmer, J., Kuhlemeyer, R.L. (1969) Finite Dynamic Model for Infinite Media, Journal of the Engineering Mechanics Division, ASCE 95 pp. 859-877.
Ministerio de Fomento/ Puertos del Estado. (2008) Geotechnical Recommendations for the Design of Maritime and Harbour Works. ROM 0.5-05. [English version]
Newmark, N.M. (1965) Effects of earthquakes on dams and embankments. Fifth Rankine Lecture. Géotechnique, 15(2), pp. 139-160.
PIANC (2001) Seismic Design Guidelines for Port Structures. International Navigation Association. Balkema, Rotterdam.
Seed H.B., and Whitman R.V. (1970) Design of earth retaining structures for dynamic loads. ASCE Special Conference on Lateral Stresses in the ground and the design of earth retaining structures, Cornell, New York, ASCE. pp. 103-147
Steedman R.S. (1998), Seismic design of retaining walls. Proc. Instn Civ. Engrs Geotech. Engng, 131, pp. 12-22.
Steedman R.S., Zeng X. (1990) The influence of phase on the calculation of pseudo-static earth pressure on a retaining wall. Géotechnique 40, No. 1, pp. 103-112.
Steedman, R.S., Zeng, X. (1996) Rotation of large gravity walls on rigid foundations under seismic loading. ASCE Geotechnical Special Publication No. 60. ASCE, Reston VA. pp. 38-56.
Wood, J.H. (1973) Earthquake Induced Soil Pressures on Structures. Report No. EERL 73-05, Earthquake Engineering Research Laboratory, Calif. Inst. Tech., Pasadena, CA.